Two Nonlinear Control Approaches for Retrieval of a Thrusting Tethered Subsatellite

D. J. Pines* and A. H. von Flotow†
Massachusetts Institute of Technology, Cambridge, Massachusetts 02139
and
D. C. Redding‡
Charles Stark Draper Laboratory, Cambridge, Massachusetts 02139

This paper presents an analysis of the dynamics and control of the pitch and roll motion during retrieval of a Tethered Satellite System, consisting of the Space Shuttle Orbiter and the tethered satellite. Two nonlinear control designs are investigated and compared. The first approach uses visual observation of the line-of-sight angle and phase-plane switch logic to generate simple rules for orbiter pilots. The second uses a controller designed using computational sliding mode techniques. It assumes more precise sensing of system state, and would be implemented using subsatellite jets.

Introduction

RETRIEVAL of a Tethered Satellite System (TSS) subsatellite is unstable in nearly all modes of motion,[1] including the simplest pitch and roll attitude motion, the tether length motion, and tether deformation. Fortunately, many of these modes are slow or weak or both. Some can be successfully stabilized by control of tether reel-in-rate for most of the retrieval.[2] Within about 2 km, however, this technique leads to very slow retrievals, and pitch and roll stabilization may be more effectively performed by using tether-normal thruster firings on one of the satellites. This is the problem we consider in this paper.

For the purpose of control design, we assume that the length motion is stabilized by a reel-in controller, which will track a specified length-rate profile. We also assume that thruster firings will not excite unstabilizable tether shape motion. This assumption is based upon the fact that the tether shape motion is subject to much faster dynamic time scales than the pitch and roll motion and the intuition that the excited tether motion will quickly return to the equilibrium shape. This allows us to treat the system as a changing-length rigid body, giving second-order unstable nonlinear equations for pitch and roll motion. We devise simple control laws using phase-plane analysis to show that these motions can be effectively and efficiently stabilized,[3] and compare these control laws to those derived with application of a design procedure termed sliding mode control.[4]

Simplified Tether Dynamics

Much of the interesting dynamics of two small satellites connected by a taut, low-mass, long tether are described by three equations describing length, pitch, and roll of the system (the center of gravity of the system is in a circular orbit):

$$\ddot{L} = L\left[(\dot{\theta}+\omega)^2\cos(\phi)+(\dot{\phi})^2+3\omega^2\cos^2(\theta)\cos^2(\phi)-\omega^2\right] + u_L \tag{1a}$$

$$\ddot{\theta} = (\dot{\theta}+\omega)2\tan(\phi)\dot{\phi} - 2(\dot{L}/L)(\theta+\omega) - 3\omega^2\cos(\theta)\sin(\theta) + u_\theta \tag{1b}$$

$$\ddot{\theta} = -2(\dot{L}/L)\dot{\phi} - \left[(\dot{\theta}+\omega)^2+3\omega^2\cos^2(\theta)\right] \times \cos(\phi)\sin(\phi) + u_\phi \tag{1c}$$

where L is the instantaneous length, θ the in-plane angle between the (straight) tether and the local vertical, ϕ the out-of-plane angle between the (straight) tether and the local vertical, and ω the orbital rate (circular orbit). Corresponding accelerations due to control efforts are represented by u_L, u_θ, and u_ϕ.

To understand the basic instabilities during retrieval, it is instructive to partially linearize these equations. It is well not to assume that the pitch angle θ remains small since it is directly driven by length changes. For $\dot{\theta}$, $\dot{\phi} \ll \omega$, $\phi \ll 1$,

$$\ddot{L} = L\left[(\dot{\theta}+\omega)^2+\omega^2\left(3\cos^2(\theta)-1\right)\right] + u_L \tag{2a}$$

$$\ddot{\theta} = -2(\dot{L}/L)(\dot{\theta}+\omega) - 3\omega^2\cos(\theta)\sin(\theta) + u_\theta \tag{2b}$$

$$\ddot{\phi} = -2(\dot{L}/L)\dot{\phi} - \left[(\dot{\theta}+\omega)^2+3\omega^2\cos^2(\theta)\right]\phi + u_\phi \tag{2c}$$

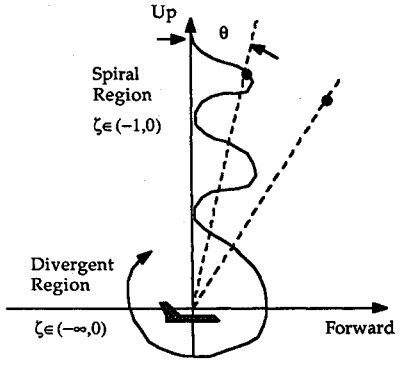

Fig. 1 In-plane projection onto the locally vertical/horizontal reference frame of a typical trajectory during open-loop retrieval.

Presented as Paper 88-4171 at the AIAA Guidance, Navigation, and Control Conference, Minneapolis, MN, Aug. 15-17, 1988; received Aug. 25, 1988; revision received Feb. 1, 1989.

*Graduate Research Assistant, Department of Aeronautics and Astronautics.
†Associate Professor, Department of Aeronautics and Astronautics.
‡Member of Technical Staff.

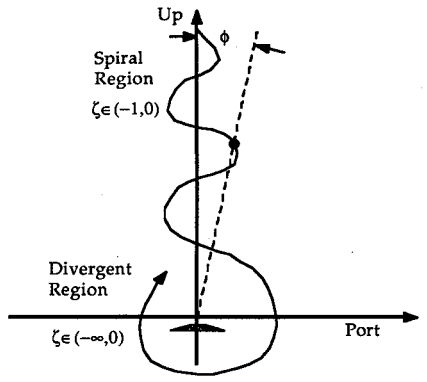

Fig. 2 Out-of-plane projection onto the locally vertical/horizontal reference frame of a typical trajectory during open-loop retrieval.

If the length is controlled so that $\dot{L}<0$, (retrieval), then the $\dot{L}/L$ term in the pitch and roll equations is negative, and both pitch and roll are negatively damped, nonlinear, second-order oscillators. There is still a small coupling from pitch into roll.

The most interesting dynamics occur in pitch. Two competing mechanisms drive the equilibrium ($\ddot{\theta}=\dot{\theta}=0$). Gravity gradient provides a torque restoring the configuration to the local vertical. Coriolis acceleration drives θ, depending on the product $\omega\dot{L}/L$. For low enough relative length rates, equilibrium is given by

$$\theta_{\text{equil}} \doteq 2\dot{L}/3L\omega \qquad \text{(valid for } \theta_{\text{equil}} \ll 1) \tag{3}$$

and during retrieval the pitch angle oscillates with growing amplitude about this equilibrium. We call this the spiral region.

For too large a relative length rate, Coriolis acceleration overcomes gravity gradient, and no equilibrium is achieved, so that $|\theta(t)|$ is an increasing function of time. We term this the divergent region.

Length Control

Tether length is directly controllable with the reel-deployer in the Orbiter payload bay. This control authority is subject to the important physical constraint that the tension remain positive, that is, that $u_L<0$.

Pitch/Roll Control

Equations (1a–1c) [or (2a–2c)] can be integrated forward in time for particular retrieval rates $L(t)$. The result is a set of trajectories of the subsatellite with respect to the Orbiter; one for each set of initial conditions. These trajectories are three-dimensional; typically their inplane or out-of-plane projections are displayed. Figure 1 is a sketch of the inplane component of typical trajectories; Fig. 2 represents the out-of-plane. The local vertical/horizontal reference frame is shown for reference.

Much of the past work[5] has focused on the possibility of controlling both pitch θ and roll ϕ via modifications in length rate $\dot{L}$. (An equivalent alternative is to control tether tension.) Although this can be very successful for long tethers, simulations have demonstrated that such an approach will not lead to feasible retrieval times if it is to be employed all the way to docking. At a distance of approximately 2 km (variable among simulations), the tether goes slack. The Italian/American TSS has tether-aligned cold gas thrusters that can help keep tension positive for a longer time,[2] however, even with the operation of these thrusters, tension controlled retrieval to $L=10$ m must be prohibitively slow. The limitation is due to the weak nature of gravity gradient torque. Such a retrieval exploits only this torque to remove the excess angular momentum as the system mass moment of inertia is reduced during retrieval.

To continue retrieval beyond 2 km at reasonable rates, it is necessary to introduce a new technique of applying external torques. If Orbiter translational maneuvers are used, the control accelerations in Eqs. (1a–1c) or (2a–2c) become

$$u_L = A_L + \text{accelerations due to the reel} \tag{4a}$$

$$u_\theta = A_\theta/L \tag{4b}$$

$$u_\phi = A_\phi/L \tag{4c}$$

where A_L is the component of the Orbiter acceleration parallel to the tether, A_θ is perpendicular to the tether and in-plane, and A_ϕ is perpendicular to the tether and out-of-plane.

The Orbiter primary reaction control system (PRCS) is not the ideal thruster system, suffering from cross-axis coupling, attitude/translation coupling and control granularity. We ignore cross-axis coupling but address granularity. The accelerations A_θ and A_ϕ are thus to be achieved by thrusting with the PRCS, whereas A_L is to be avoided. In this analysis, A_ϕ and A_θ are assumed to be 1.0 ft/s^2 and $A_L=0$. The control angular accelerations, u_θ and u_ϕ are thus equal to 1.5×10^{-4} rad/s^2 for $L=2$ km, and increasing for shorter lengths. Angular accelerations during pitch and roll librations of the uncontrolled system, in low-Earth orbit ($\omega=0.001$ rad/s) are approximately $\ddot{\theta}_{\max}$, $\ddot{\phi}_{\max}=2.0\times10^{-6}$ rad/s^2 for $\theta_{\max}$, $\phi_{\max}=30$ deg. Control accelerations are thus at least two orders of magnitude greater than the natural open-loop accelerations. There is plenty of control authority.

Phase Plane Analysis

For initial control design, it is instructive to look at the pitch dynamics on a phase plane. This is best done for various constant values of $\dot{L}/L$. Since $\dot{L}/L$ is time varying, the actual phase-plane trajectories will be a continuously changing blend of those we show here.

Inspection of Eq. (2b), and comparison with the standard form for the second-order linear oscillator equation

$$\ddot{\theta} + 2\zeta\omega_n\dot{\theta} + \omega_n^2\theta = f(t) \tag{5}$$

suggests that the pitch motion will consist of growing oscillations with frequency

$$\omega_n = \sqrt{3}\omega \tag{6}$$

and with envelope given by

$$e^{-\zeta\omega_n t}; \qquad \zeta = \dot{L}1/L_\omega\sqrt{3} \tag{7}$$

This viewpoint remains valid for slow length changes, $|\zeta| \ll 1$, but, for rapid retrieval or for short lengths, the motion changes character; the pitch angle diverges monotonically in time. The boundary between these motions is given approximately by

$$\dot{L}/L \approx -\omega\sqrt{3} \tag{8}$$

Figure 3 shows phase-plane trajectories of the solution to Eq. (2b), integrated numerically, for $\dot{L}/L=-0.0005$ s^{-1} corresponding to a retrieval rate of $\dot{L}=-1$ m/s and a length of $L=2000$ m. The spirals closely resemble those obtained for a fully linearized analysis as long as the pitch angle θ, remains small.

Figure 4 shows the same phase plane trajectories for a faster relative retrieval, $\dot{L}/L=-0.005$ s^{-1}, corresponding to $\dot{L}=-1$ m/s at $L=200$ m. Note that the pitch angle grows either in a negative or positive sense, depending on initial conditions. The time constant of this exponential growth is approximately $\dot{L}/L$.

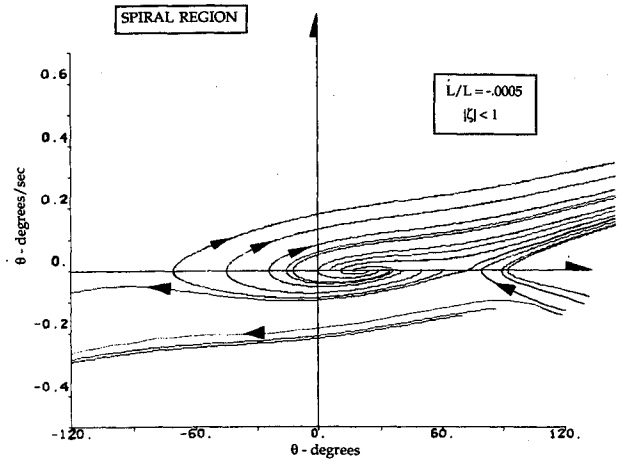

Fig. 3 Phase plane portrait of pitch motion for slow relative retrieval rate; spiral region.

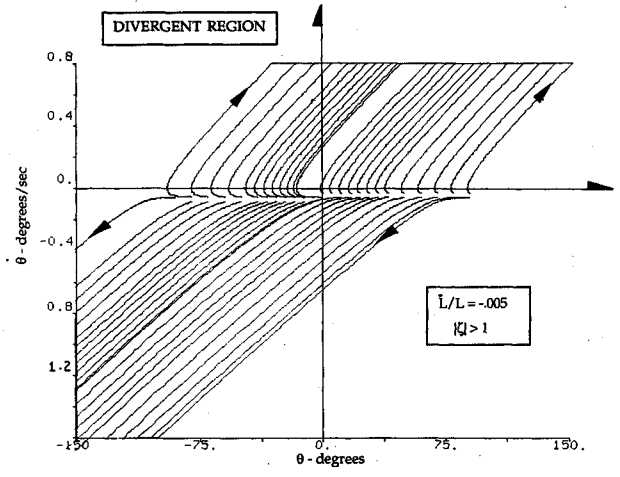

Fig. 4 Phase plane portrait of pitch motion for fast relative retrieval rate; divergent region.

Open-Loop Control with the Tether Reel

From this analysis it is clear that the open-loop behavior is unstable. Even then, it is interesting to visualize a family of unstable equilibrium trajectories $\theta(t)$, $L(t)$, each from a particular initial condition. One can define a guidance problem by proposing to use the tether reel to enforce a length time history $L(t)$, which results in desirable final conditions $\theta(t_f)$, $\phi(t_f)$ when the length arrives at the docking length. This length time history is subject to implementation constraints; one certainly cannot push with the tether. A reasonable objective function to be minimized may be the final time, although we anticipate having to impose an upper limit on the retrieval rate. We have not solved this guidance problem. Rather, we have quite arbitrarily specified a retrieval rate beginning at $\dot{L} = -1$ m/s at an initial length of 2 km, decreasing linearly to $\dot{L} = -0.5$ m/s at a final length of 10 m. This leads to a retrieval time of 44 min. Even for this length time history, initial conditions exist that lead to retrieval at or near zero pitch angle and zero pitch rate. Figure 5 is a plot of one such trajectory, found by trial and error. Also shown is a trajectory that begins from very similar initial conditions but diverges; the reference trajectory is unstable.

Although open-loop retrieval is impractical, trajectories similar to those sketched in Fig. 5 might form the basis of a future feedforward/feedback control scheme. Each initial condition would generate its own reference trajectory, to be implemented with the tether reel. The tether-normal thrusters would be used for feedback, firing occasionally to stabilize this reference motion. The remainder of this paper addresses the feedback control; we leave the issues of solving for good length time histories $L(t)$ for further research, and in computed results use the 44 min retrieval described in the prior paragraph.

Pilot-in-the-Loop Feedback

Pitch Control Design

Our basic objective is to generate a set of pilotage rules for the Orbiter pilot to follow. These will be something like, "when the subsatellite moves 30 deg ahead of the Orbiter, input a "0.5 ft/s $\Delta(V)$." This control is to be implemented by a human pilot at the aft flight deck, with visual access to the payload bay and overhead. It is important that these rules be carefully derived and analyzed, in order to assure stability and fuel efficient control.

Within the 2-km point the tethered satellite should be in the view of a pilot looking up from the Orbiter's aft flight deck. With the aid of some system instrumentation it is likely that the Orbiter crew could measure the line of sight to the tethered subsatellite (from which line-of-sight rate could also be estimated). Combined with Orbiter attitude information, this could provide estimates of θ and ϕ usable to manually stabilize a rapid retrieval. Control would be provided by the Orbiter's PRCS jets activated from the aft flight deck by the pilot following pilotage rules such as those derived in this section.

The subsequent paragraphs develop a bang-bang control logic in which the reference trajectory is much cruder than discussed in the prior section:

$$\theta_r = \text{const} \tag{9}$$

This approach reflects our perception of the precision achievable with pilot-in-the-loop bang-bang control.

The phase-plane trajectories followed when the PRCS is firing can be approximated as very steep parabolas, since the normalized control torque is a very large number,

$$\tau = A_\theta / 3\omega^2 L \tag{10}$$

easily overpowering the rate terms in the pitch equation. This suggests a simple control law, as sketched in Fig. 6.

The objective here is to keep within a region defined by a reference angle θ_r and a dead band zone angle θ_c. The lines at the edge of this region are switch lines. If a trajectory hits the $\theta = \theta_r + \theta_c$ switch line from the left, a negative pitch firing (a translation firing for the Orbiter) is indicated. This firing will push θ slightly past the $\dot{\theta} = 0$ line, putting the system on a slow

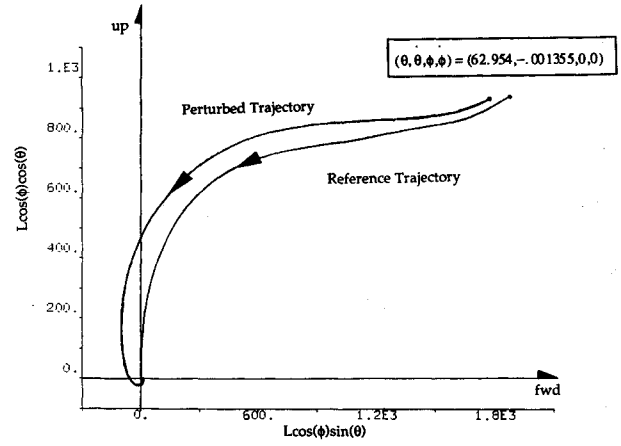

Fig. 5 Two in-plane open-loop trajectories from nearly the same initial conditions. The reference trajectory approaches docking with small pitch angle and rate, while the perturbed trajectory wraps around the Orbiter.

coasting arc back through $\dot{\theta}=0$ and around towards the same switch line, in a slow, one-sided limit cycle (spiral region); or on a faster path towards the other switch line, setting up a two-sided limit cycle (divergent region).

This approach works if $\dot{L}/L$ is constant, in either the spiral or divergent regions. It also works if $\dot{L}/L$ is not held constant, as can be demonstrated by simulation.

The performance of the phase-plane approach will depend on achieving accurate burn shut-off conditions. The ideal burn will just reverse $\dot{\theta}$.

Pitch Control Examples

Two example retrievals (from 2 km to 10 m) are presented using the dynamics of Eq. (1b), which model the Orbiter and tethered satellite as point masses. Retrieval rate at the initial length of 2 km was -1 m/s; retrieval rate decreases linearly in magnitude so that at the end (44 min later), it is -0.5 m/s. Orbiter thrust acceleration is 0.3 m/s^2. All firings are shut off when $\dot{\theta}$ is driven below -0.01 deg/s, with a 2 s granularity. Docking is defined to occur when the tether length reaches $L=10$ m.

The first example sets the reference θ_r at 0 deg, with a 30 deg deadband (see Fig. 7). It shows one limit cycle firing in the spiral region; the second occurs when the tether is quite short, and divergent motion starts just prior to "capture" at $L=10$ m. Capture occurs at a pitch angle of 2 deg and pitch rate of -0.30 deg/s. Total Orbiter ΔV was 2.7 m/s, for about 350 lb of fuel.

The second example differs from the first by having $\theta_c=50$ deg rather than 30 deg (see Fig. 8). Three burns are done; the first during spiral motion, the second during divergent motion, and the third occurs just prior to capture. Total ΔV was 3 m/s. This case was hurt by the granularity (2 s) of the jet firings, which forced the motion onto a more divergent path than desired after the last firing. Capture in this simulation occurs at a pitch angle of 50 deg and a pitch rate of -0.2 deg/s.

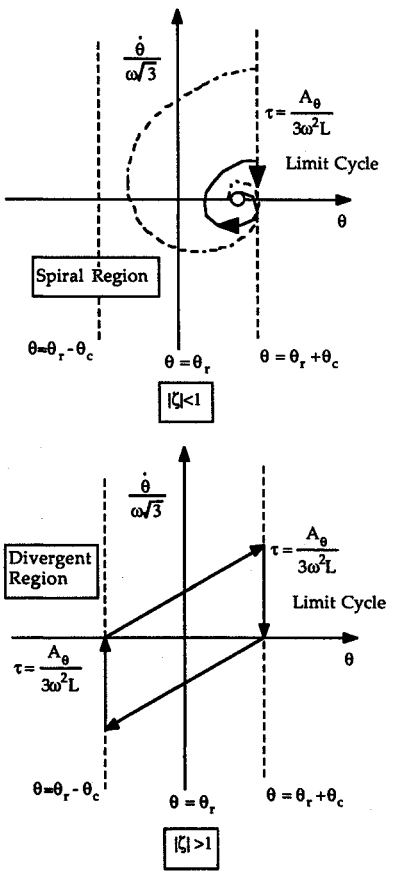

Fig. 6 Phase plane switching lines for large control effort, and two types of resulting limit cycles. The limit cycle will be either slow and one-sided (spiral region) or faster and two-sided (divergent region).

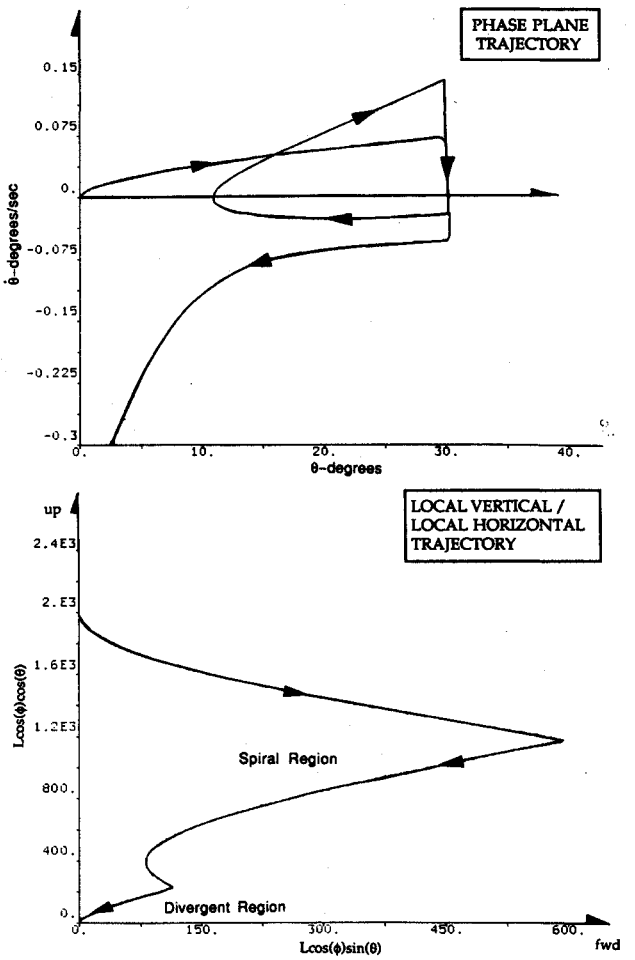

Fig. 7 Phase plane and local-vertical/local-horizontal controlled retrieval trajectories with in-plane motion only. The switching lines of Fig. 6 have been implemented, with $\theta_c=30$ deg, $\theta_r=0.0$.

A number of other runs were made, varying all parameters of the problem. Results show that the performance, as measured by ΔV for retrieval, are sensitive to θ_r, θ_c, reel-in rate $\dot{L}$, and especially to the burn shut-off point. The worst cases, with ΔV up to 60 m/s, were for tight control (small θ_c) with slow reel-in rates. Further analysis to define the best retrieval length trajectories, and hence the best control laws, is required.

Roll Control Design

The roll dynamics are less interesting than the pitch dynamics in that the Coriolis force is lacking. Inspection of Eq. (2c) reveals a second-order non-linear oscillator, either damped or undamped according to $\dot{L}/L$, but with equilibrium at $\phi=0$. During retrieval the roll angle is an oscillatory growing function of time and becomes nonoscillatory divergent for retrievals exceeding

$$\dot{L}/L=-2\omega \tag{11}$$

The phase-plane trajectories in roll are thus very similar to those plotted in Figs. 3 and 4, the essential differences being that the equilibrium roll angle remains zero.

This suggests switching lines in roll equivalent to those in pitch, with $\phi_r=0$ and ϕ_c perhaps 20 deg. The Orbiter is accelerated out-of-plane to generate the system roll acceleration. The resulting limit cycle involves two burns, and is symmetric about $\phi=0$, but otherwise resembles the limit cycles of Fig. 6. Although we do not show simulated results, similar performance and fuel consumption can be expected in roll as was reported in pitch.

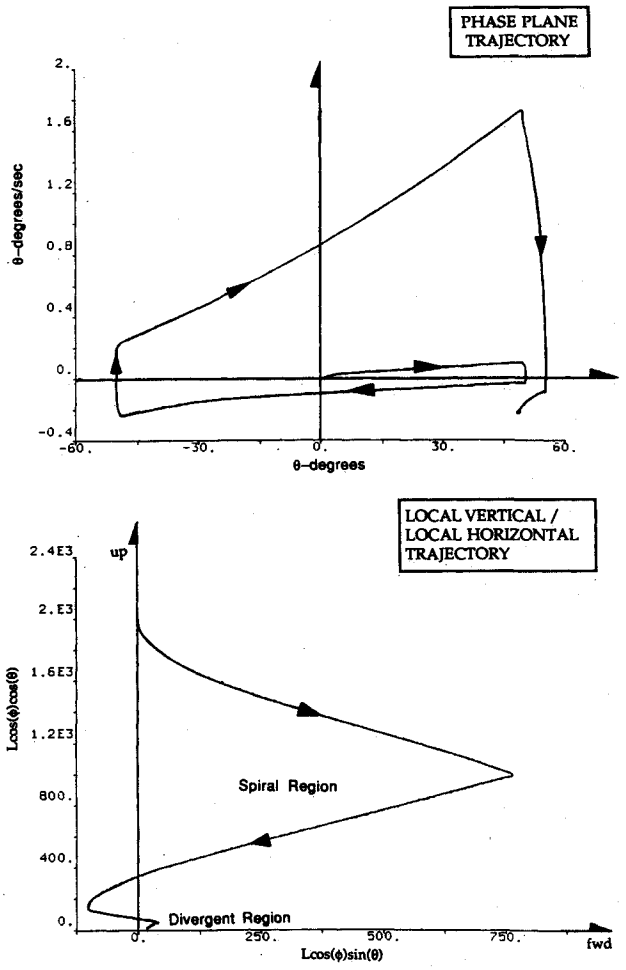

Fig. 8 Phase plane and local-vertical/local-horizontal controlled retrieval trajectories with in-plane motion only. The switching lines of Fig. 6 have been implemented, with $\theta_c = 50$ deg.

Automatic Control

The preceding paragraphs have sketched a control approach strongly influenced by the explicit assumption that the control would be implemented with a human pilot in the loop. This assumption has had the influence that the approach taken makes minimal demands on sensing precision and on pilot input timing. Although it is likely that the preceding approach could be refined, still retaining the pilot in the loop, we elect rather to investigate an alternative approach that would require automatic loop closure but that promises higher performance. Concomitant demands are placed on sensing and actuation; it appears that implementation of such control would require the development of a much more capable subsatellite.

Sliding Mode Approach

The dynamics defined by Eqs. (1) and (2) are inherently nonlinear. Furthermore, if one specifies the length time history $L(t)$, then the pitch and roll dynamics become nonlinear with time-varying coefficients. A nonlinear control design procedure is thus called for. One such procedure, with increasing recent popularity, is known as sliding mode control. This method involves the notion of a surface in state space[6]; nonlinear control laws are derived that drive the state to this surface and then along the surface to the desired state. Previous application of this method to unstable nonlinear problems resulted in the specification of large control authority and high frequency chatter. The concept of the boundary layer, developed by Slotine and Sastry,[7] appears to have removed this unwanted behavior and is directly comparable to the deadband and hysteresis classically used in bang-bang control design in the phase plane.

In this section, we develop sliding mode controllers for both pitch and roll dynamics, and compare them to the previous phase-plane designs. These controllers are allowed to become more complex than the preceding designs, reflecting the perception that they will be implemented in closed loop. One complication we investigate is the specification of a time-varying commanded pitch reference angle θ, chosen to represent an unstable equilibrium solution of the pitch equation of motion (presented in Fig. 5).

As before, we assume that a reel-in controller forces the length to track a specified length profile; the same 44 min retrieval used in the preceding section. Following the lead of others,[4] we define element sliding surfaces S_θ and S_ϕ as

$$S_\theta = \dot{e}_\theta + \lambda_\theta e_\theta \tag{12}$$

$$S_\phi = \dot{e}_\phi + \lambda_\phi e_\phi \tag{13}$$

where $e_\theta = \theta - \theta_d$, $e_\phi = \phi - \phi_d$, and λ_θ and λ_ϕ are parameters that influence the dynamics on the sliding surfaces S_θ and S_ϕ, respectively. The element surfaces in Eqs. (12) and (13) are thus decoupled, however, this may not always be desirable.

If we diffentiate these element surfaces and combine them with Eq. (1) we have

$$\dot{S}_\theta = (\dot{\theta}+\omega)\,2\tan(\phi)\dot{\phi} - 2(\dot{L}/L)(\dot{\theta}+\omega) - 3\omega^2\cos(\theta)\sin(\theta) - \ddot{\theta}_d + \lambda_\theta(\dot{\theta}-\dot{\theta}_d) + u_\theta \tag{14}$$

$$\dot{S}_\phi = -(\dot{L}/L)\phi - \left[(\theta+\omega)^2 + 3\omega^2\cos^2(\theta)\right]\cos(\phi)\sin(\phi) + u_\phi \tag{15}$$

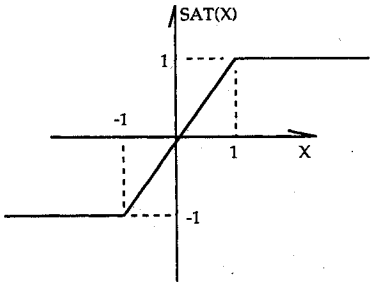

Fig. 9 Saturation function.

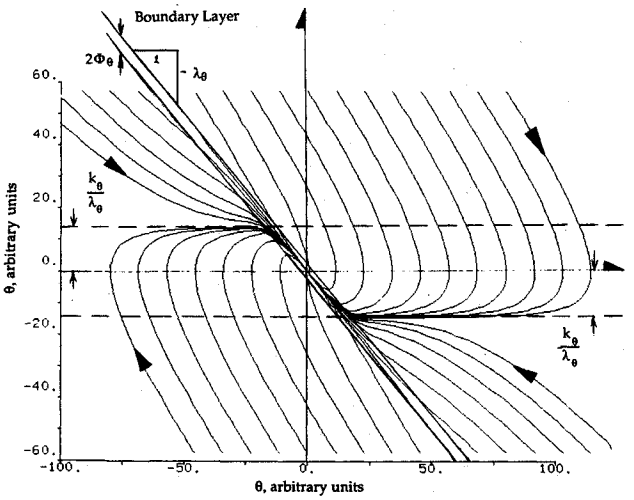

Fig. 10 Closed-loop trajectories in the phase plane with perfect implementation of sliding mode control.

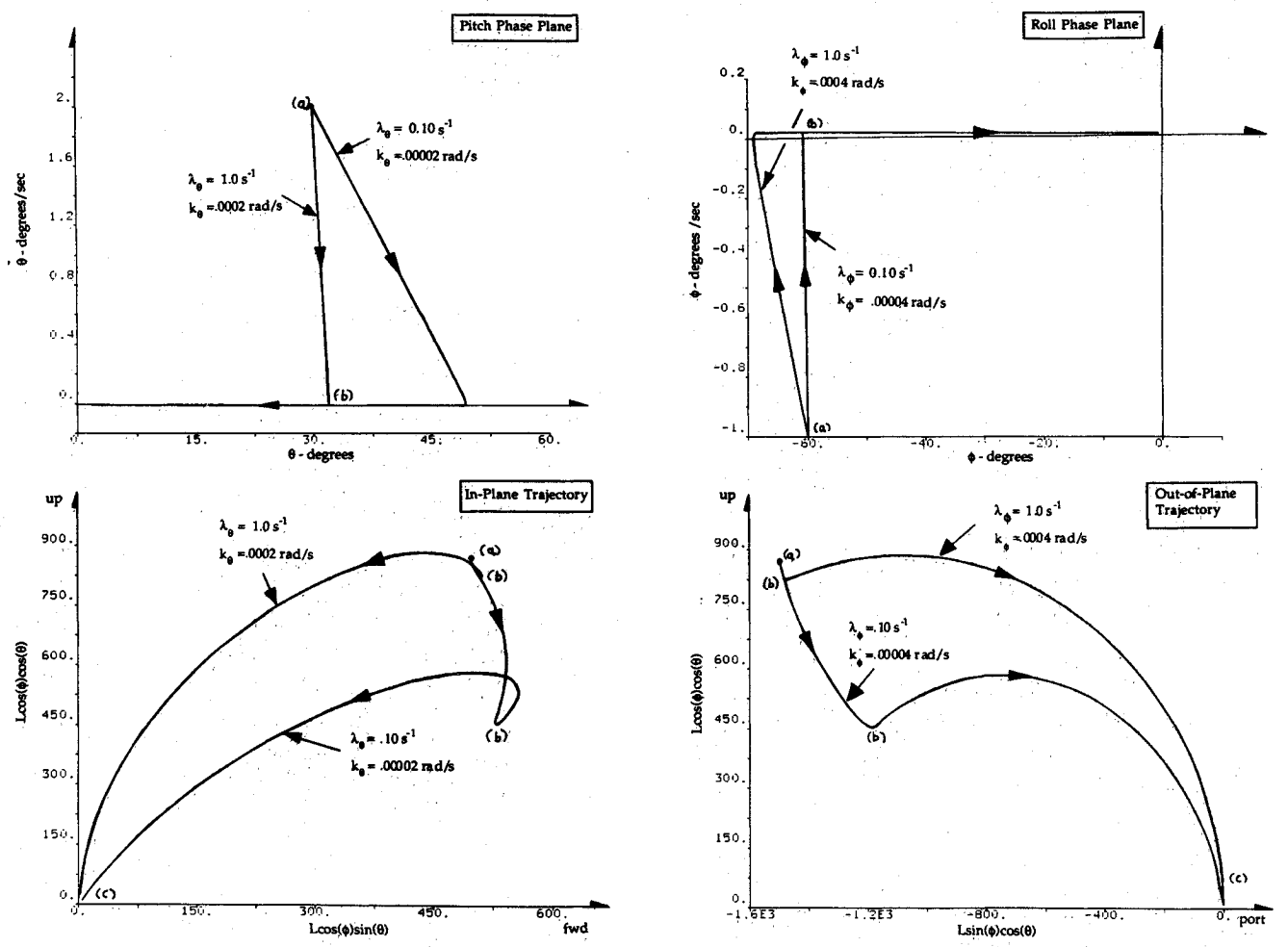

Fig. 11 Two closed-loop trajectories with ideal sliding mode control. Trajectories are started from an arbitrary initial condition in roll and in pitch.

The control law is based on

$$\dot{S}_\theta = -k_\theta \,\mathrm{sat}(S_\theta) \tag{16a}$$

$$\dot{S}_\phi = -k_\phi \,\mathrm{sat}(S_\phi) \tag{16b}$$

where use of the saturation function, sat(x) follows the lead of Ref. 4, and is done to suppress control chatter (see Fig. 9). Alternative switching functions might be used. This choice has no effect on the closed-loop trajectories, except when sliding along the sliding surface, in which case details of the deadband will strongly influence chatter and thrusting frequency.

The control law is chosen to satisfy the following attractiveness relations

$$\frac{1}{2}\frac{\mathrm{d}}{\mathrm{d}t}(S_\theta^2) < -k_\theta |S_\theta| \tag{17a}$$

$$\frac{1}{2}\frac{\mathrm{d}}{\mathrm{d}t}(S_\phi^2) < -k_\phi |S_\phi| \tag{17b}$$

where k_θ and k_ϕ represent controller gains.

Combining Eqs. (14–17) leads to the following two nonlinear equations governing the control acceleration for both pitch and roll motion

$$u_\theta = -\Big[(\dot{\theta}+\omega)2\tan(\phi)\dot{\phi} - 2(\dot{L}/L)(\dot{\theta}+\omega) - 3\omega^2\cos(\theta)\sin(\theta) - \ddot{\theta}_d + \lambda_\theta(\dot{\theta}-\dot{\theta}_d) + k_\theta \,\mathrm{sat}(S_\theta)\Big] \tag{18}$$

$$u_\phi = -\Big[-(\dot{L}/L)\phi - \Big[(\theta+\omega)^2 + 3\omega^2\cos^2(\theta)\Big]\cos(\phi)\sin(\phi) - \ddot{\phi}_d + \lambda_\phi(\dot{\phi}-\dot{\phi}_d) + k_\phi \,\mathrm{sat}(S_\phi)\Big] \tag{19}$$

Equations (20) and (21) represent nominal nonlinear controllers for pitch and roll control.

At this point we can summarize this control scheme in the phase plane. Let's concentrate on pitch behavior only, by suppressing roll; $\phi = 0$.

The sliding surface can be seen to be an inclined line in the pitch phase plane, with slope $= -\lambda_\theta$ (see Fig. 10). Notice that the dashed parallel lines in this figure correspond to the saturation function, which defines a boundary region about the sliding surface. The nonlinear feedforward terms in the control acceleration u_θ specified by Eq. (18) have the effect of reducing the closed-loop pitch dynamics to

$$\Delta\ddot{\theta} = -\lambda_\theta\Delta\dot{\theta} - k_\theta \,\mathrm{sat}\{S_\theta/\Phi_\theta\} \tag{20}$$

where $\Delta\theta = \theta - \theta_d$ is the pitch angle error. Error trajectories are sketched in Fig. 10. Because of the nonlinear feed-forward term in the control, the natural dynamics are completely suppressed. The closed-loop dynamics for roll are thus the same as those for pitch. Even the nonlinear roll-yaw coupling is suppressed by the control specification of Eq. (19). Implementation issues of such control are discussed in a subsequent section.

Sliding Mode Examples

These examples are computed using actuation without restriction to on-off, discrete control. We discuss implementation issues in a subsequent section. The first example considers retrieval of the subsatellite from an arbitrary initial condition in roll and pitch. The dynamics of this response are illustrated in Fig. 11. As evident from this figure the sliding mode con-

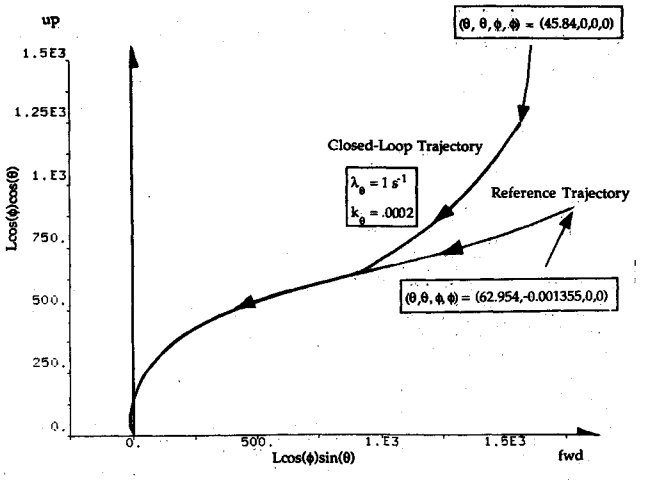

Fig. 12 Sliding mode control of a perturbed trajectory toward a reference trajectory that represents equilibrium motion. The reference trajectory is unstable.

trollers direct the pitch and roll phase-plane trajectories toward the sliding surfaces S_θ and S_ϕ. Once on the surface, small control effort is expended. A boundary layer specified by $\Phi_\phi = \Phi_\theta = 0.0005$ rad/s prevents chatter.

The second example investigates the use of an unstable equilibrium trajectory as a reference trajectory for feedback control. The equilibrium trajectory of Fig. 5 is replotted, as is a closed-loop trajectory from different initial conditions. The sliding mode controller quickly drives the error to zero, and the two trajectories track one another without further control effort (see Fig. 12). In implementation, one would of course not expect such perfect behavior.

On/Off Implementation of Sliding Mode Control

As seen in Figs. 11 and 12, the sliding mode control procedure avoids control chatter but specifies continuously varying levels of thrust. Most spacecraft thrusters are on-off devices; continuous thrust levels are approximated by fast pulsing with pulse width and pulse frequency (PWPF) modulation.[8] We thus have the logical inconsistency of avoiding high-frequency chatter, but introducing some thrust pulsing.

To reasonably approximate the effect of continuous thrusting, the pulsing interval must be short compared to the system characteristic times; in this example a reasonable upper bound for the pulsing interval is 5 min. A 44-min retrieval thus might require 10 thrust pulses, suggesting that much of the fine detail and smoothness of the calculated closed-loop trajectories will be destroyed. Typical spacecraft thrusters are also constrained with respect to the minimum duration thrust pulse. For the Orbiter, a minimum PRCS pulse results in a velocity increment of approximately 0.1 ft/s. The minimum average thrust-induced acceleration of the Orbiter is thus approximately $A_{\min} = 1.0 \times 10^{-4}$ m/s^2. This leads to a minimum angular acceleration u_θ and u_ϕ, which depends on length;

$$u_{\min} = A_{\min}/L \tag{21}$$

and suggests that the Orbiter PRCS is capable of providing the small average angular accelerations demanded by the sliding mode controller near the end of the retrieval. Further study with Orbiter and autopilot simulation software is necessary to verify this tentative conclusion.

The ultimate hardware solution would involve the development of a subsatellite with much greater control capability than the orbiter. Thrusting on the subsatellite is much more fuel efficient than thrusting on the Orbiter, simply because of the disparity in mass. Proportional thrusters appear necessary to properly implement sliding mode control.

Unmodeled Effects

Although these two approaches to control design seem quite promising, a detailed dynamic model is required to verify our results before definitive flight procedures will be possible. Some of the specific assumptions that must be addressed are as follows:

1) Orbiter translational accelerations are uncoupled. The Orbiter is actually incapable of performing a pure translational maneuver with its reaction control system. Instead, rotation is excited, leading to unwanted accelerations of the tether attach point.

2) Tether longitudinal and transverse motion are negligible. Sudden translational accelerations of the Orbiter will excite tether motion. A detailed simulation would investigate the impact of this response.

3) Estimation of Orbiter/subsatellite motion. Since the rate of change of pitch and roll behavior of the TSS is on the order of orbital rate, system attitude rate will have to be approximated by visual observation of the system attitude. Errors may lead to unnecessary overshoot or undershoot in the control.

4) Control design at docking. Based solely on safety precautions, it is conceivable that the control strategy used here might have to be radically changed during the final phase of retrieval when the subsatellite is near the Orbiter.

Summary

This paper has applied two approaches to nonlinear control design to the problem of stabilizing retrieval of a tethered subsatellite via thrusting. The two approaches differ enormously in their design process and in their closed-loop behavior.

Phase Plane Control Design

The first approach, based on line-of-sight trajectories, leads to a simple control logic to be implemented by the Orbiter pilot. Visual observation of subsatellite line-of-sight angle together with Orbiter state knowledge are expected to be adequate to assure stable retrieval by this approach. Performance is characterized by limit cycling behavior which changes with retrieval rate and tether length. The Orbiter's thrusters are used in a small number of relatively long duration burns to maintain the slow limit cycles.

Sliding Mode Control

The second approach applies an algorithm for control design of nonlinear systems to this system. This algorithm, sliding mode control, is of general applicability and thus makes it difficult to exploit known dynamics behavior of the system. The procedure requires full-state feedback and specifies continuously varying thrust level. If these thrust levels are approximated by thruster pulsing, a moderate number of thruster burns are required.

A logical extension to the sliding mode approach would be to define a broad deadband zone about the sliding surface of the equilibrium trajectory to reduce the number of thruster firings. Conceptually this is identical to the first approach implemented about the equilibrium trajectory with switch lines set at the limit of the boundary-layer dead-band zone. Further implementation-motivated modifications of the sliding mode control procedure may drive it toward an even stronger similarity with the phase plane design.

References

[1]Xu, D. M., Misra, A. K., and Modi, V. J., "On Thruster Augmented Active Control of a Tethered Sub-Satellite System During its Retrieval," AIAA Paper 84-1993, Aug. 1984; also, Ph.D. Thesis, McGill Univ., Montreal, Quebec, Canada, 1984.

[2]Crouch, D. S., and Vignoli, M. M., "Shuttle Tethered Satellite System Development Program," AIAA Paper 84-1106, June 1984.

[3]von Flotow, A., Redding, D., and Stuart, D., "Control of Tethered Satellite System Retrieval by Orbiter Translation Maneuvers," C. S. Draper Lab., Cambridge, MA, Memo SSV-85-15, March 1986.

[4]Fernandez, B. R., and Hedrick, J. K., "Control of Multivariable Non-Linear Systems by the Sliding Mode Method," *International Journal of Control,* Vol. 46, No. 3, 1987, pp. 1019–1040.

[5]Misra, A. K., and Modi, V. J., "A Survey on the Dynamics and Control of Tethered Satellite Systems," NASA/AIAA/PSN International Conference on Tethers in Space, Arlington, VA, Sept. 1986.

[6]Utkin, V. I., "Sliding Modes and their Application in Variable Structure Systems," Translated from the Russian by A. Parnakh (Moscow: MIR); 1984. *Automn Remote Control,* Vol. 44, p. 1105.

[7]Slotine, J. J. E., and Sastry, S. S., "Sliding Controller Design for Non-Linear Systems," *International Journal of Control,* Vol. 40, No. 2, pp. 421–434.

[8]Wie, B., and Plescia, C. T., "Attitude Stabilization of Flexible Spacecraft During Stationkeeping Maneuvers," *Journal of Guidance, Control, and Dynamics,* Vol. 7, No. 4, July–Aug. 1984, pp. 430–436.